BNL-103689-2014-TECH

AGS/RHIC/SN 064;BNL-103689-2014-IR

Rotation Angle of a Helical Dipole

T. Tominaka

September 1997

Collider Accelerator Department

Brookhaven National Laboratory

U.S. Department of Energy

USDOE Office of Science (SC)

DISCLAIMER

Alternating Gradient Synchrotron Department
Relativistic Heavy Ion Collider Project
BROOKHAVEN NATIONAL LABORATORY
Upton, New York 11973

Spin Note

AGS/RHIC/SN No. 64

Rotation Angle of a Helical Dipole

Toshiharu Tominaka

AGS Department, Brookhaven National Laboratory, NY 11973

September 22, 1997

Rotation Angle of a Helical Dipole

T. Tominaka (RIKEN, Japan)

September 8, 1997

1 INTRODUCTION

The relation between the rotation angle and the cancellation of the integral of transverse field along the beam axis is investigated. First of all, the simple optimization method for the full-size helical dipoles is studied on the assumption of the linearized relation for the beam axis coordinate dependence of the dipole field and the phase of the dipole field. In this analysis, the optimum length of the helical dipole is calculated as a function of the phase changing rate of dipole in the end, which can not be simply predicted. This optimization method is not so accurate for the real estimation, but it is understandable and effective for the rough estimation.
Secondly, the optimization method for the helical dipoles with the known end is studied. Actually, the optimized length for the full-size helical dipoles is obtained for the measured field of the prototype helical coil. In addition, the field integral along the beam axis is estimated for the full-size helical dipoles consisting of the optimized helical body portion and the non-symmetric ends of the prototype helical coil.

2 DEFINITION OF THE ROTATION ANGLE FOR HELICAL DIPOLES

Though the dipole field of helical dipole coils rotates, the effective magnetic length, L, can be defined in the similar manner with the conventional 2-dimensional dipole.

$$L = \frac{1}{B_1(z=0)} \int_{-\infty}^{+\infty} B_1(z)\, dz = \frac{1}{B_{10}} \int B_1(z)\, dz \quad , \tag{1}$$

where $B_1(z)$ is the intensity of the dipole field at z, and $B_{10} = B_1(z=0)$ is the intensity of dipole field at the center. As a natural extension of this effective magnetic length due to the replacement of the z coordinate by the angle, φ, the effective magnetic rotation angle, $\Delta\varphi$, can be defined similarly as follows,

$$\Delta\varphi = \frac{1}{B_1(\varphi=0)} \int_{-\infty}^{+\infty} B_1(\varphi)\, d\varphi = \frac{1}{B_{10}} \int B_1(\varphi)\, d\varphi \quad , \tag{2}$$

where $B_1(\varphi)$ is the intensity of the dipole field at the angle, $\varphi(z)$, with the definition of $\varphi(z=0)=0$, and $B_{10} = B_1(\varphi=0) = B_1(z=0)$. Eq.(2) can be rewritten as a function of z as follows,

$$\Delta\varphi = \frac{1}{B_{10}} \int B_1(\varphi(z)) \frac{d\varphi}{dz} dz = \frac{1}{B_{10}} \int B_1(\varphi(z)) \frac{d\varphi}{dz} dz = \overline{\frac{d\varphi}{dz}} L \quad . \tag{3}$$

In this definition, it means that the magnetic field where $d\varphi/dz = 0$ does not contribute to the effective magnetic rotation angle.

3 RELATION BETWEEN THE ROTATION ANGLE AND THE CANCELLATION OF THE TRANSVERSE INTEGRATED FIELD

In general, the integral of the field component, B_a for the arbitrary direction with the angle, φ_0 for the y axis, can be expressed as follows,

$$\int B_a(z)\, dz = \int B_1(\varphi(z)) \cos(\varphi(z) - \varphi_0)\, dz = 0 \quad , \tag{4}$$

which may be rearranged to give

$$\left\{ \int B_1(\varphi(z)) \cos\varphi(z)\, dz \right\} \times \cos\varphi_0 + \left\{ \int B_1(\varphi(z)) \sin\varphi(z)\, dz \right\} \times \sin\varphi_0 = 0 \quad . \tag{5}$$

Then, the following equations must be fulfilled to meet the condition for the arbitrary direction,

$$\begin{cases} \int\int B_1(\varphi(z)) \cos\varphi(z)\, dz = \int B_y(z)\, dz = 0 \\ \int\int B_1(\varphi(z)) \sin\varphi(z)\, dz = -\int B_x(z)\, dz = 0 \end{cases} . \tag{6}$$

Then, it can be realized that the cancellation of the integral of the field component, B_a for the arbitrary direction is equivalent to those for two transverse direction, x and y direction. In addition, ideally, $B_x(z)$ can be defined to be an odd function from the symmetry for the magnet center, z=0, with $B_x(z=0)=0$. Therefore, the integral of the x-directional field, B_x is always zero for every helical magnet,

$$\int B_x(z)\, dz = 0 . \tag{7}$$

As a result, it is realized that the cancellation of the integral of the y-directional field, B_y is essential for that of the integral of the field component, B_a for the arbitrary direction.

$$\int B_y(z)\, dz = \int B_1(\varphi(z)) \cos\varphi(z)\, dz = \int B_1(\varphi(z)) \cos\varphi(z) \frac{dz}{d\varphi} d\varphi = 0 . \tag{8}$$

3.1 In the case of the perfect helical dipole without the end-field effect

For the case of the perfect helical dipole with the rotation angle of 2π (the integration $-\pi$ to π), with $B_1(\varphi(z)) = B_{10}$ = constant, $d\varphi/dz = k$ = constant, the Eq.(8) become simply the following form, showing that the 2π rotation corresponds to the cancellation of the integral of the y-directional field, B_y.

$$\int_0^{\pi} B_1(\varphi(z)) \cos\varphi(z) \frac{dz}{d\varphi} d\varphi = \frac{B_{10}}{k} \int_0^{\pi} \cos\varphi \; d\varphi = 0 . \tag{9}$$

3.2 In the case of $d\varphi/dz = k$ = constant with the end-field effect

With the following simple end field,

$$\begin{cases} B_1(z) = B_1(z=0) = B_{10}, & 0 \le z \le \frac{L}{2} - \frac{\delta}{2} \\ B_1(z) = -\frac{B_{10}}{\delta}\left\{ z - \frac{L}{2} - \frac{\delta}{2} \right\}, & \frac{L}{2} - \frac{\delta}{2} < z < \frac{L}{2} + \frac{\delta}{2} \end{cases} , \tag{10}$$

where $B_1(z)$ is assumed to decrease linearly to zero in the end region. The integral of the y-directional field, B_y can be written in the following form,

$$\int_0^{\frac{L}{2}+\frac{\delta}{2}} B_y(z)\, dz = \int_0^{\frac{L}{2}-\frac{\delta}{2}} B_1(z) \cos\varphi(z)\, dz + \int_{\frac{L}{2}-\frac{\delta}{2}}^{\frac{L}{2}+\frac{\delta}{2}} B_1(z) \cos\varphi(z)\, dz . \tag{11}$$

The contribution from the helical body portion can be calculated as follows,

$$\int_0^{\frac{L}{2}-\frac{\delta}{2}} B_1(z) \cos\varphi(z)\, dz = \int_0^{\pi-\varepsilon} B_1(\varphi(z)) \cos\varphi(z) \frac{dz}{d\varphi} d\varphi = \frac{B_{10}}{k} \int_0^{\pi-\varepsilon} \cos\varphi \, d\varphi = \frac{B_{10}}{k} \sin\varepsilon , \tag{12}$$

where $\varphi((L-\delta)/2) = k(L-\delta)/2 = \pi - \varepsilon$ is defined. From the end portion,

$$\int_{\frac{L}{2}-\frac{\delta}{2}}^{\frac{L}{2}+\frac{\delta}{2}} B_1(z)\cos\varphi(z)\,dz = -\frac{B_{10}}{\delta}\int_0^{\delta}(z-\delta)\cos(kz+\pi-\varepsilon)\,dz$$

$$= -\frac{B_{10}}{\delta}\left\{-\frac{\cos(\varepsilon-k\delta)}{k^2}+\frac{\cos\varepsilon+k\delta\sin\varepsilon}{k^2}\right\} \quad . \tag{13}$$

If $k\delta$ is equal with 2ε ($k\delta=2\varepsilon$), the cancellation can be obtained,

$$\int_{\frac{L}{2}-\frac{\delta}{2}}^{\frac{L}{2}+\frac{\delta}{2}} B_1(z)\cos\varphi(z)\,dz = -\frac{B_{10}}{k}\sin\varepsilon = -\int_0^{\frac{L}{2}-\frac{\delta}{2}} B_1(z)\cos\varphi(z)\,dz \quad . \tag{14}$$

The effective rotation angle of this case can be calculated from Eq.(3),

$$\Delta\varphi = \frac{2}{B_{10}}\int_0^{\frac{L}{2}+\frac{\delta}{2}} B_1(z)\frac{d\varphi}{dz}dz = 2(\pi-\varepsilon)+\frac{2}{B_{10}}\int_{\frac{L}{2}-\frac{\delta}{2}}^{\frac{L}{2}+\frac{\delta}{2}} B_1(z)\frac{d\varphi}{dz}dz$$

$$= 2(\pi-\varepsilon)+\frac{2}{B_{10}}\int_0^{\delta}-\frac{B_{10}}{\delta}(z-\delta)\,k\,dz = 2(\pi-\varepsilon)+k\delta = 2\pi \quad . \tag{15}$$

In this case, it is verified that the cancellation of integrated field is equivalent to the effective rotation angle of 2π, which is equal to the rotation angle between the magnetic length from z=-L/2 to L/2.

3.3 In the case of $d\varphi/dz = ke \neq k$ at the end-field region

In the following case that the rate of the phase rotation in the end region, k_e, is different from that in the helical body part,

$$\begin{cases} B_1(z) = B_1(z=0) = B_{10}, & \dfrac{d\varphi}{dz} = k, & 0 \le z \le \dfrac{L}{2}-\dfrac{\delta}{2} \\ B_1(z) = -\dfrac{B_{10}}{\delta}\left\{z-\dfrac{L}{2}-\dfrac{\delta}{2}\right\}, & \dfrac{d\varphi}{dz} = k_e, & \dfrac{L}{2}-\dfrac{\delta}{2} \le z \le \dfrac{L}{2}+\dfrac{\delta}{2} \end{cases} , \tag{16}$$

the contribution from the end portion can be calculated as follows,

$$\int_{\frac{L}{2}-\frac{\delta}{2}}^{\frac{L}{2}+\frac{\delta}{2}} B_1(z)\cos\varphi(z)\,dz = -\frac{B_{10}}{\delta}\int_0^{\delta}(z-\delta)\cos(k_e z+\pi-\varepsilon)\,dz$$

$$= -\frac{B_{10}}{\delta}\left\{-\frac{\cos(\varepsilon-k_e\delta)}{k_e^2}+\frac{\cos\varepsilon+k_e\delta\sin\varepsilon}{k_e^2}\right\} \quad . \tag{17}$$

Then, the angle ε can be obtained as a function of k_e and δ from the following equation required for the cancellation of the integrated B_y field.

$$\frac{\sin\varepsilon}{k}-\frac{1}{\delta}\left\{-\frac{\cos(\varepsilon-k_e\delta)}{k_e^2}+\frac{\cos\varepsilon+k_e\delta\sin\varepsilon}{k_e^2}\right\} = 0 \quad . \tag{18}$$

In addition, the rotation angle of this case become,

$$\Delta\varphi = \frac{2}{B_{10}}\int_0^{\frac{L}{2}+\frac{\delta}{2}} B_1(z)\frac{d\varphi}{dz}dz = 2(\pi - \varepsilon) + k_e\delta = 2(\pi - \varepsilon) + \frac{2}{B_{10}}\int_0^{\delta} -\frac{B_{10}}{\delta}(z - \delta)\, k_e\, dz = 2\pi - (2\varepsilon - k_e\delta) \quad . \tag{19}$$

Therefore, for the cancellation of integrated transverse field, the effective rotation angle should be reduced from 2π by the angle $2\varepsilon - k_e\,\delta$.
Especially, in the case of $k_e = 0$, the requirement for the integrated B_y becomes,

$$\int_0^{\frac{L}{2}+\frac{\delta}{2}} B_y(z)\,dz = \int_0^{\frac{L}{2}-\frac{\delta}{2}} B_1(z)\cos\varphi(z)\,dz + \int_{\frac{L}{2}-\frac{\delta}{2}}^{\frac{L}{2}+\frac{\delta}{2}} B_1(z)\cos\varphi(z)\,dz$$

$$= \frac{B_{10}}{k}\sin\varepsilon + \cos(\pi - \varepsilon)\int_0^{\delta} -\frac{B_{10}}{\delta}(z - \delta)\,dz = \frac{B_{10}}{k}\sin\varepsilon - \frac{B_{10}\,\delta}{2}\cos\varepsilon = 0 \quad . \tag{20}$$

Then, the following relation is obtained from the above equation,

$$\varepsilon = \tan^{-1}\left(k\frac{\delta}{2}\right) \quad . \tag{21}$$

The effective rotation angle, $\Delta\varphi$, also becomes,

$$\Delta\varphi = 2\pi - 2\varepsilon = 2\pi - 2\tan^{-1}\left(k\frac{\delta}{2}\right) \quad . \tag{22}$$

3.4 In the case with the realistic (or measured) end-field region

In the following case with the realistic end region,

$$\begin{cases} B_1(z) = B_1(z=0) = B_{10}, & \dfrac{d\varphi}{dz} = k, & 0 \le z \le z_e \\ B_1(z) = B_{10}\, b(z - z_e), & \varphi = \varphi(z - z_e), & z_e \le z \le z_f \end{cases} \quad , \tag{23}$$

where the function $b(z-z_e)$ describes the z dependence of the normalized dipole field, and function $\varphi(z-z_e)$ also describes the z dependence of the phase of the dipole field. The following equation is required to meet the condition of the zero integrated transverse field,

$$\int_0^{z_f} B_y(z)\,dz = \int_0^{z_e} B_1(z)\cos\varphi(z)\,dz + \int_{z_e}^{z_f} B_1(z)\cos\varphi(z)\,dz = 0 \quad , \tag{24}$$

which may rearrange to give,

$$B_{10}\int_0^{z_e} \cos(k\,z)\,dz + \int_0^{z_f - z_e} B_1(z - z_e)\cos\left[\varphi(z - z_e) + k\,z_e\right]dz = 0 \quad . \tag{25}$$

Then, the half length of the helical body portion, z_e is required to meet the following equation,

$$\int_0^{z_f - z_e} b(z - z_e)\cos\left[\varphi(z - z_e) + k\,z_e\right]dz = -\frac{\sin(k\,z_e)}{k} \quad . \tag{26}$$

The above equation can be solved numerically.

4 MEASURED RESULTS OF THE BNL PROTOTYPE HELICAL MAGNET

The z dependence of the dipole field, $B_1(z)$, the phase of dipole field, $\varphi(z)$, and the phase changing rate, $d\varphi(z)/dz$, which was obtained from the magnetic measurement with Hall probe are shown in Figs.1 - 3 for I=105 A and in Figs.4 - 6 for I=220 A, respectively.[1,2,3] In these figures, the central position of the magnet, z = 0, is defined as the middle point for the magnetic length. The z dependence of the dipole field, $B_1(z)$, and the phase of dipole field, $\varphi(z)$, are roughly approximated with δ = 0.2 m, k = 150 deg/m, k_e = 75 deg/m, L = 1.195 m (for 105 A) or 1.191 m (for 220 A) on Eq.(16). This linearly approximated curves for both of the dipole field, $B_1(z)$, and the dipole phase, $\varphi(z)$, are shown in Figs.1 - 2 for I=105 A and in Figs.4 - 5 for I=220 A. The z dependence of the normalized dipole field, $B_1(z)/B_{10}$, and the dipole phase, $\varphi(z)$, for both end regions are also shown in Figs.7 - 8 for I=105 A and in Figs.9 - 10 for I=220 A, respectively with z_e = 0.4 m. The difference of the magnetic structures in both ends seems to be little. The rotation angles for the body portion and end potions are listed in Table 1. In Table 1, $\Delta\varphi$ [left], $\Delta\varphi$ [body], and $\Delta\varphi$ [right] mean the rotation angles for the left end potion, the body portion, and the right end portion.

In addition, it seems that the thermal contraction of helical dipole can be detected through the estimation of the effective magnetic length, L, (=1.200 m at room temperature) and the changing rate of the phase of dipole field between z = - 0.4 m and z = 0.4 m, k = $d\varphi/dz$ (=150 deg/m at room temperature) as shown in Table 1. The estimated results is almost consistent to the expected thermal contraction of Al coil bobbin of 0.415 % from the room temperature to 4.2 K.

Table 1 Comparison between the prototype and the simulated full-size helical magnet

	L (m)	k (deg/m)	$\Delta\varphi$ [total] (deg)	$\Delta\varphi$ [left] (deg)	$\Delta\varphi$ [body] (deg)	$\Delta\varphi$ [right] (deg)
Prototype (105 A)	1.195	150.7	166.6	22.7	120.3	23.6
Prototype. (220 A)	1.191	150.4	166.8	23.0	120.4	23.4
Full-size (Linear Model)	2.401	150.0	345.2	15.0*	315.2*	15.0*
Full-size (Symmetric)	2.401	150.0	348.3	23.4	301.5	23.4
Full-size (Symmetric)	2.391	150.6	348.0	23.4	301.2	23.4
Full-size (Non-symmetric)	2.390	150.6	347.6	23.0	301.2	23.4

5 CALCULATION FOR A HELICAL MAGNET WITH FULL LENGTH

5.1 Linear Aproximation

First of all, for the nominal rate of the phase rotation in the helical body part, k = 150 (deg/m), and three values, 0.1 m, 0.2 m, and 0.3 m of the length of end regions, δ, the effective rotation angle, $\Delta\varphi$, can be calculated as a function of the rate of the phase rotation on the end region, k_e, from Eqs.(18), (19), (21), and (22), as shown in Fig.13. Especially, the effective rotation angle, $\Delta\varphi$, and the effective magnetic length, $L = \Delta\varphi/k + \delta\,(1 - k_e/k)$, solved for the above-mentioned values, $k = 2\pi/2.4$ (rad/m) = 150 (deg/m), $k_e = k/2$ = 75 (deg/m), and δ = 0.2 m, are listed in Table 1. In this case, $\Delta\varphi$ [left], and $\Delta\varphi$ [right] correspond to the length of the end region, δ = 0.2 m, differently from the other case listed in Table 1.

5.2 In the Case with the End of Half Length Prototype Magnet

With the assumption of the symmetric magnetic structure that both ends are identical, and are the same with the end of the prototype helical magnet from z = + 0.4 m to z = + 0.8 m, shown in Figs.9 - 10 for I=220 A, and k = 150 (deg/m) for the helical body part, the half body length, z_e can be calculated from Eq.(26), obtaining z_e = 1.005 m. This means that the helical body portion of the prototype magnet from z = - 0.4 m to z = + 0.4 m, should be replaced by that with the length, 1.005 × 2 = 2.01 m for the full-size magnet, resulting on the extension of the helical body portion of (1.005 - 0.4) × 2 = 1.21 m. In addition , the following results are listed in Table 1,

the effective rotation angle : $\Delta\varphi = 23.4 \times 2 + 150.0 \times 2 \times 1.005 = 348.3$ (deg) , and,
the effective magnetic length : L = 2.401 (m).

This result seems to be almost equivalent to that calculated by TOSCA.[4] Similarly, in the case of k = $2\pi/\{2.4 \times (1 - 0.00415)\}$ (rad/m) = 150.6 (deg/m), the half body length, z_e can be also calculated, obtaining $z_e = 1.000$, and the following values, as listed in Table 1.

the effective rotation angle : $\Delta\varphi = 23.4 \times 2 + 150.6 \times 2 \times 1.000 = 348.0$ (deg) , and,
the effective magnetic length : L = 2.391 (m).

Furthermore, with the assumption of the non-symmetric magnetic structure that each end is different, and the same with the each end from z = - 0.8 m to z = - 0.4 m or from z = + 0.4 m to z = + 0.8 m, shown in Figs.9 - 10 for I = 220 A, and for the same helical body part with k = 150.6 (deg/m), the non-symmetric full-size helical dipole can be constructed, as lastly listed in Table 1. For B_{10} = 4.0 T, the field distribution of this non-symmetric full-size helical dipole are shown in Figs.14 - 20. In these figures, black dots are shown at every 5.0 mm along the beam axis for the indication of the relation between the same z positions in each figure. Especially, the distribution of the field component, B_a for the direction with the angle, $\varphi_0 = +30$ degree for the y axis is shown in Fig.19. The comparison for the integral of the magnetic field between the symmetric and non-symmetric ends of the last two cases listed in Table 1, is shown in Table 2.[4,5] It can be checked that the integral of B_a is the same with that calculated from the integral of B_x, and B_y, using Eqs(4), (5), (6).

Table 2 The integrated vales of the magnetic field along the beam axis

	Integral of B_x (Tm)	Integral of B_y (Tm)	Integral of B_a (Tm) [$\varphi_0 = 30$ deg]
Symmetric	0	-2.2×10^{-6}	-1.9×10^{-6}
Non-symmetric	$+1.5 \times 10^{-3}$	$+5.8 \times 10^{-4}$	-2.5×10^{-4}

6 CONCLUSION

The rotation angle of helical dipoles is defined, similarly with the magnetic length. Then, it seems to be reasonable that the rotation angle of helical dipoles is defined as that between the effective magnetic length. The relation between the rotation angle and the cancellation of the transverse integrated field depends on the magnetic structure in the end of helical dipoles. As a result, it is shown that the rotation angle of helical dipoles, which meets the condition of the cancellation of the transverse integrated field, deviates from 2π for the case that the changing rate of the rotation angle is not constant. There are some difficulties that the rotation of the dipole field is specified only by the rotation of the coil in the helical body region, whereas the field rotation in the end region is not specified only by the rotation of the coil, but also depends on the structure of the end structure of iron yoke.
As a result, it is shown that the length and the rotation angle of the helical dipoles can be optimized for the known ends. In addition, it is shown that the field integral along the beam axis for helical dipoles with the non-symmetric ends become larger than that for the symmetric ends.

7 ACKNOWLEDGMENTS

The author is indebted for providing the experimental data to A. Jain and R. Thomas, and for helpful discussions and comments to M. Okamura, E. Willen, M. Syphers, T. Roser, and T. Katayama.

REFERENCES

1) A. Jain, Private Communications.
2) R. Thomas, "Recalibration of Vertical Positions of Hall Probe Vertical Transporter", BNL Memorandum (1997).
3) M. Okamura, "The Hall Probe Measurement and Calculation of the Half Length the Helical Dipole Magnets", AGS/RHIC/SN No.60, August 20, (1997).
4) M. Okamura, "Optimization of Rotation Angle of the Helical Dipole Magnets", to be published in AGS/RHIC/SpinNotes.
5) M. J. Syphers, "Total Pitch Specification for RHIC Helical Dipole Magnets", AGS/RHIC/SN No.58, August 4, (1997).

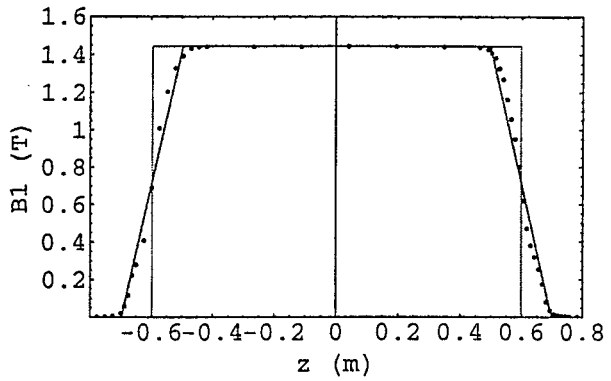

Fig.1 z dependence of the dipole field, B1(z), along the beam axis, I=105 A.

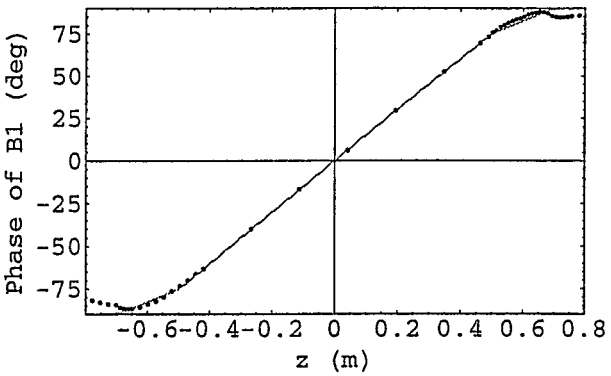

Fig.2 z dependence of the phase of the dipole field, $\varphi(z)$, along the beam axis, I=105 A.

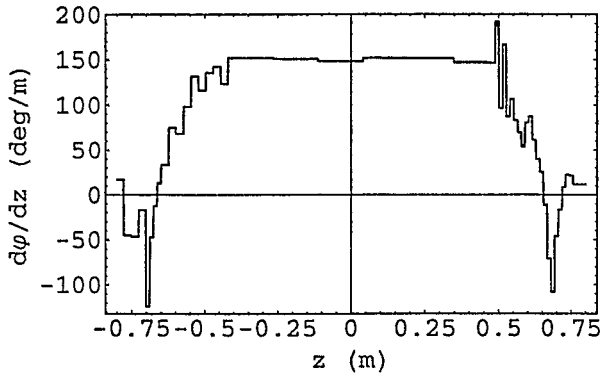

Fig.3 z dependence of the phase changing rate of the dipole field, $d\varphi(z)/dz$, along the beam axis, I=105 A.

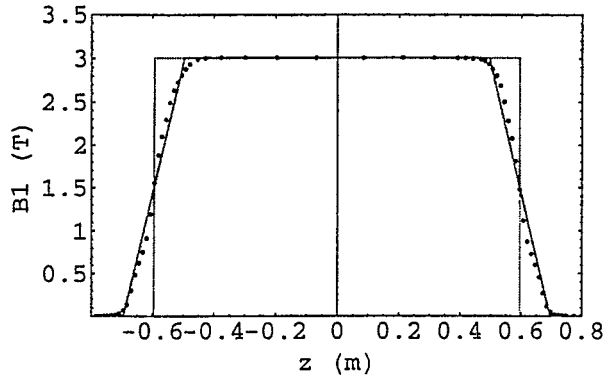

Fig.4 z dependence of the dipole field, B1(z), along the beam axis, I=220 A.

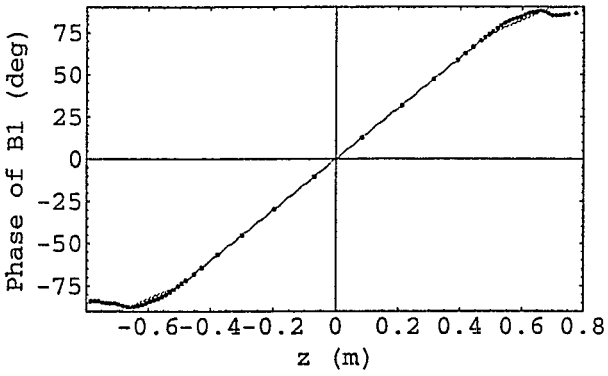

Fig.5 z dependence of the phase of the dipole field, $\varphi(z)$, along the beam axis, I=220 A.

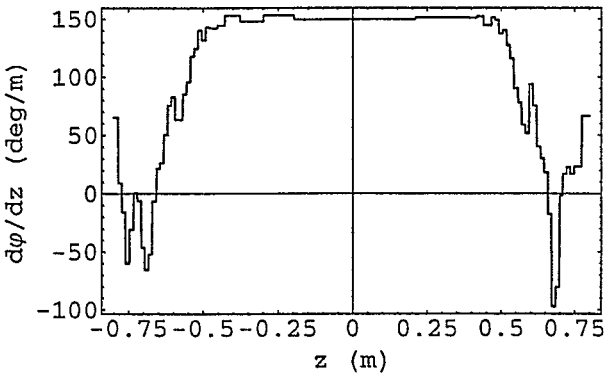

Fig.6 z dependence of the phase changing rate of the dipole field, $d\varphi(z)/dz$, along the beam axis, I=220 A.

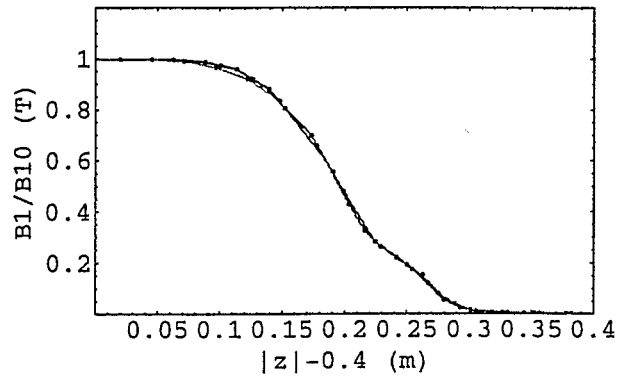

Fig.7 z dependence of the dipole field, B1(z), along the beam axis for both ends, at I=105 A.

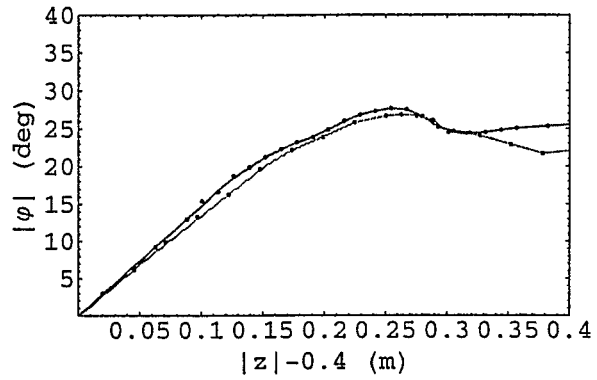

Fig.8 z dependence of the phase of the dipole field, $\varphi(z)$, along the beam axis for both ends, at I=105 A.

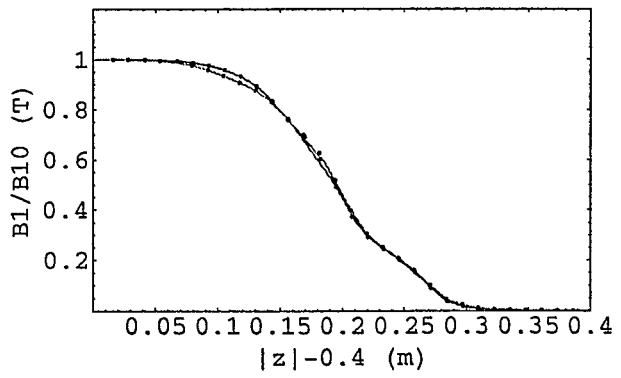

Fig.9 z dependence of the dipole field, B1(z), along the beam axis for both ends, at I=220 A.

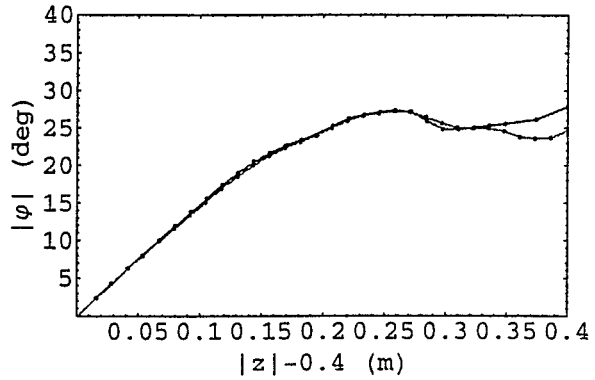

Fig.10 z dependence of the phase of the dipole field, $\varphi(z)$, along the beam axis for both ends, at I=220 A.

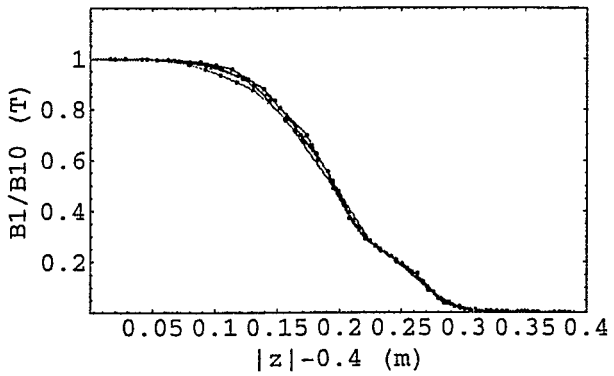

Fig.11 z dependence of the dipole field, B1(z), along the beam axis for both ends, at I=105 A and I=220 A.

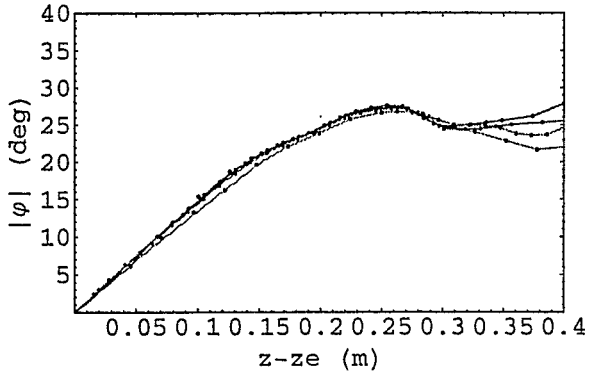

Fig.12 z dependence of the phase of the dipole field, $\varphi(z)$, along the beam axis for both ends, at I=105 A and I=220 A.

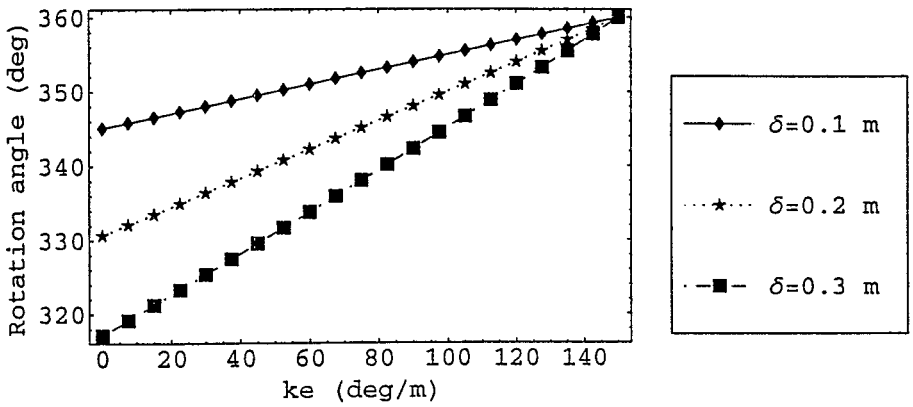

Fig.13 ke and δ dependence of the rotation angle of the dipole field, $\Delta\varphi$.

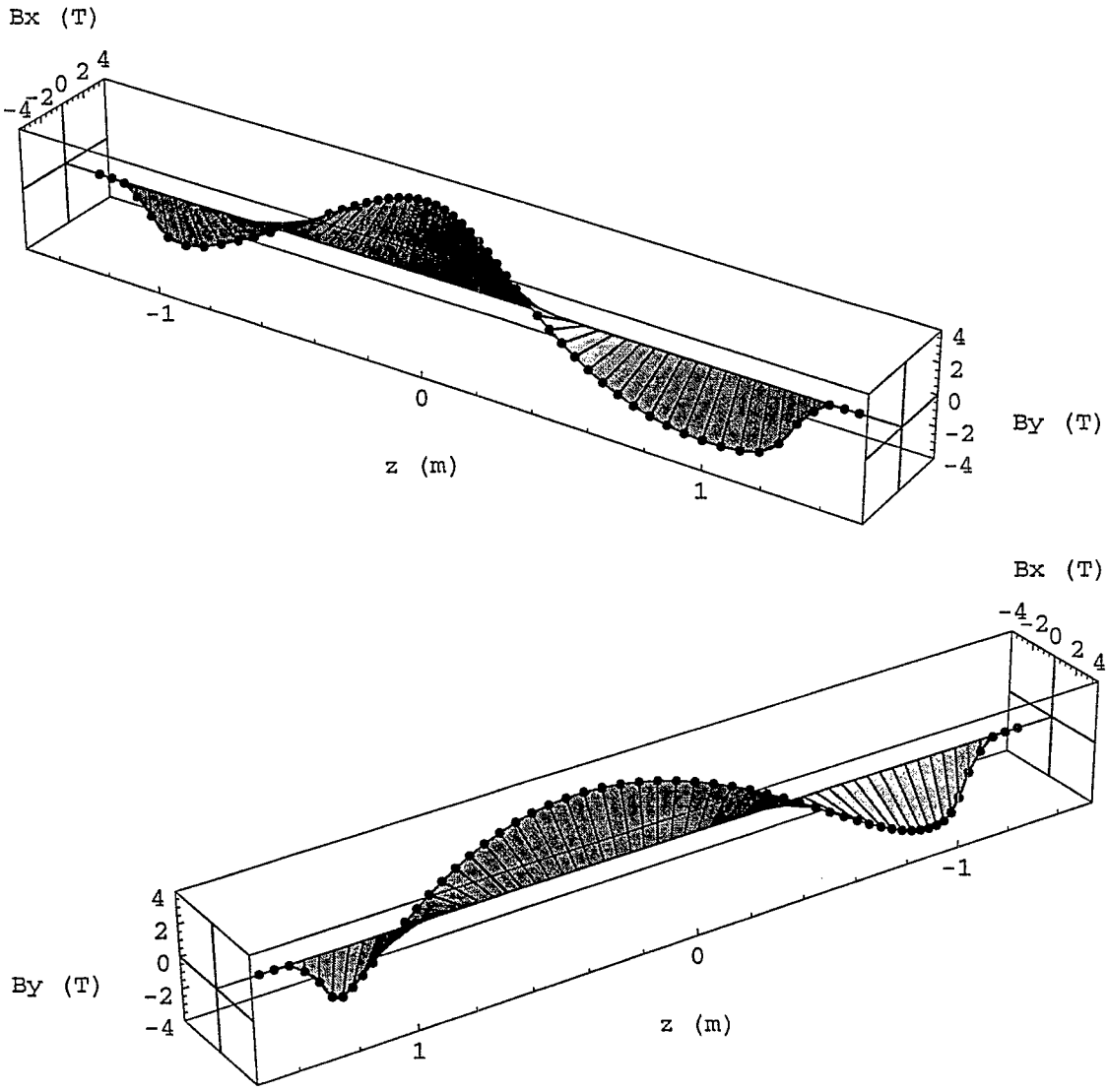

Fig.14 3D plot of the dipole field along the beam axis.

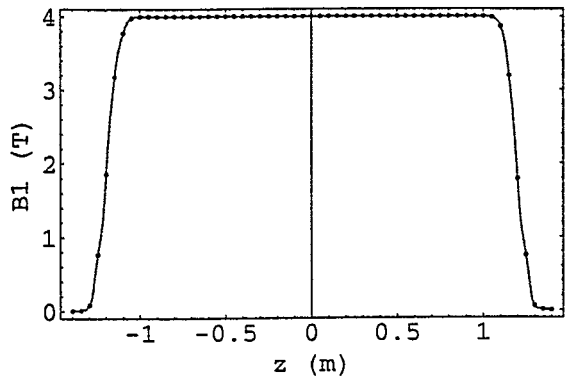

Fig.15 z dependence of the dipole field, B1(z), along the beam axis.

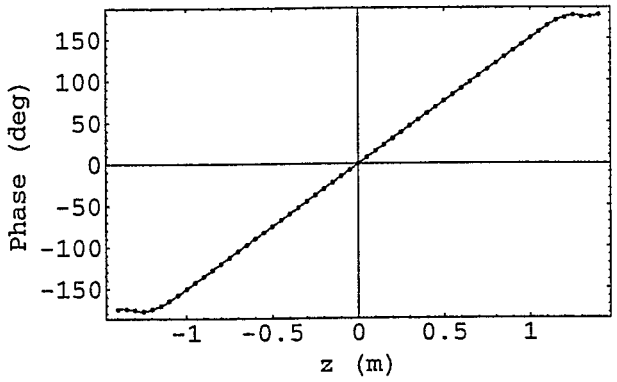

Fig.16 z dependence of the phase of the dipole field, $\varphi(z)$, along the beam axis.

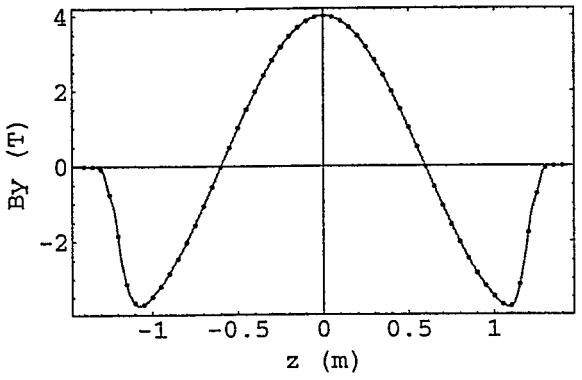

Fig.17 z dependence of By(z) along the beam axis.

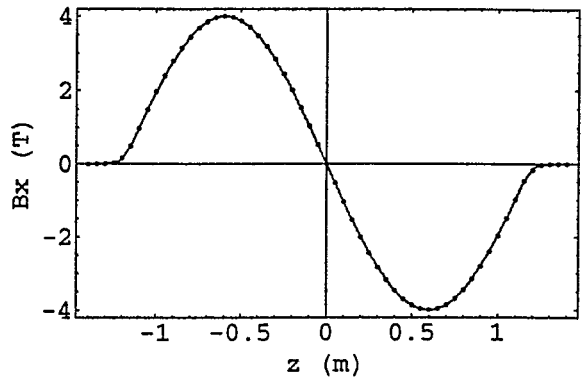

Fig.18 z dependence of Bx(z) along the beam axis.

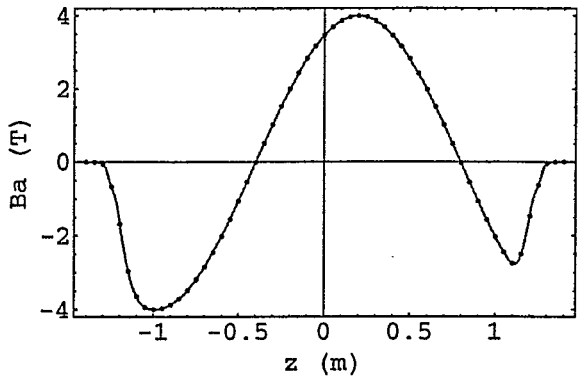

Fig.19 z dependence of field for the direction with 30 degree for the y-axis, along the beam axis.

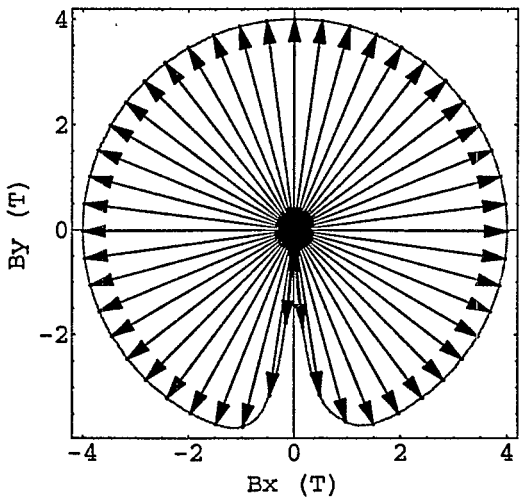

Fig.20 Plot of {Bx,By} along the beam axis.